

1 **The effect of emission source chemical profiles on simulated PM_{2.5} components:**
2 **sensitivity analysis with CMAQv5.0.2**

3 Zhongwei Luo^{a,b,1}, Yan Han^{a,b,c,1}, Kun Hua^{a,b}, Yufen Zhang^{a,b*}, Jianhui Wu^{a,b}, Xiaohui
4 Bi^{a,b}, Qili Dai^{a,b}, Baoshuang Liu^{a,b}, Yang Chen^c, Xin Long^c, Yinchang Feng^{a,b*}

5 ^aState Environmental Protection Key Laboratory of Urban Ambient Air Particulate
6 Matter Pollution Prevention and Control & Tianjin Key Laboratory of Urban
7 Transport Emission Research, College of Environmental Science and Engineering,
8 Nankai University, Tianjin 300350, China.

9 ^bCMA-NKU Cooperative Laboratory for Atmospheric Environment-Health Research,
10 Tianjin 300350, China.

11 ^cResearch Center for Atmospheric Environment, Chongqing Institute of Green and
12 Intelligent Technology, Chinese Academy of Sciences, Chongqing 400714, China.

13

14

15 *Corresponding authors:

16 Y. F. Zhang (zhafox@nankai.edu.cn). And Y. C. Feng (fengyc@nankai.edu.cn).

17

18 ¹Z. W. Luo and Y. Han equally contribute to this work

19 **Abstract**

20 The chemical transport model (CTM) is an essential tool for air quality prediction
21 and management, widely used in air pollution control and health risk assessment.
22 However, the current models do not perform very well in reproducing the observations
23 of some major chemical components, for example, sulfate, nitrate, ammonium and
24 organic carbon. Studies suggested that the uncertainties of model chemical mechanism,
25 source emission inventory and meteorological field can cause inaccurate simulation
26 results. Still, the emission source profile (used to create speciated emission inventories
27 for CTMs) of PM_{2.5} has not been fully taken into account in current numerical
28 simulation. This study aims to answer (1) Whether the variation of source profile
29 adopted in CTMs has an impact on the simulation of PM_{2.5} chemical components? (2)
30 How much does it impact? (3) How does the impact work? Based on the characteristics
31 and variation rules of chemical components in typical PM_{2.5} sources, different
32 simulation scenarios were designed and the sensitivity of simulated PM_{2.5} components
33 to source chemical profile was explored. Our findings showed that the influence of
34 source profile changes on simulated PM_{2.5} components could not be ignored.
35 Simulation results of some components were sensitive to the adopted source profile in
36 CTMs. Moreover, there was a linkage effect, the variation of some components in the
37 source profile would bring changes to the simulated results of other components. These
38 influences are connected to chemical mechanisms of the model since the variation of
39 species allocations in emission sources can affect potential composition and phase state
40 of aerosols, chemical reaction priority and multicomponent chemical balance in
41 thermodynamic equilibrium system. We also found that the perturbation of the PM_{2.5}
42 source profile caused the variation of simulated gaseous pollutants, which indirectly
43 indicated that the perturbation of source profile would affect the simulation of
44 secondary PM_{2.5} components. Given the vital role of air quality simulation in
45 environment management and health risk assessment, the representativeness and
46 timeliness of source profile should be considered.

47 **Keywords**

48 PM_{2.5}; source profile; component; numerical simulation; chemical transport model

49 **1. Introduction**

50 Ambient fine particulate matter (PM_{2.5}) pollution in some key regions of China
51 has attracted much attention (Liang et al., 2020; Huang et al., 2021). The chemical
52 components of PM_{2.5}, including elements (Al, Si, Fe, Mn, Ti, Cu, Zn, Pb, etc.), water-
53 soluble ions (SO₄²⁻, NO₃⁻, Cl⁻, F⁻, NH₄⁺, Na⁺, K⁺, Mg²⁺, Ca²⁺, etc.), and carbon-
54 containing components (Organic Carbon, OC; Elemental Carbon, EC) (Yang et al.,
55 2011; Li et al., 2013), have different physical and chemical properties, such as reactivity,
56 thermal stability, particle size distribution, residence time, optical properties, health
57 hazards, etc (Seinfeld and Pandis, 2006; Tang et al., 2006). According to long-term
58 monitoring results, in most regions of China, SO₄²⁻, NO₃⁻, NH₄⁺ and OC are the most
59 important species in ambient PM_{2.5} (Li et al., 2017a; Li et al., 2021), which has a certain
60 adverse impact on human health (Shi et al., 2018) and ecosystem, such as acid rain in
61 southwest China (Han et al., 2019), food security (Zhou et al., 2018), etc.

62 The chemical transport models (CTMs) play an important role in policy making
63 for regulatory purposes. Based on the scientific understanding of atmospheric physical
64 and chemical processes, CTMs are built to simulate the transport, reaction and removal
65 of pollutants on a certain scale in horizontal and vertical directions. With the
66 development of CTMs, the simulation accuracy of PM_{2.5} concentration has been
67 significantly improved. Higher requirements have been put forward for the precise
68 simulation of PM_{2.5} components so as to provide support for the use of CTMs in human
69 health risk assessment, climate effects, pollution sources apportionment, and so on
70 (Peterson et al., 2020; Lv et al., 2021). However, the current models perform not very
71 well in simulating some components (for example, PM_{2.5}-bound sulfate, nitrate,
72 ammonium, trace elements, etc.) (Zheng et al., 2015; Fu et al., 2016; Ying et al., 2018;
73 Cao et al., 2021). In the current literatures, the correlation coefficient (R) and
74 normalized mean bias (NMB) are highly variable and inconsistent between the
75 simulated and the observed values (listed in Table S1). This is mainly attributable to the
76 uncertainties of model chemical mechanism, source emission inventory and

77 meteorological field simulation.

78 The chemical mechanisms involved in CTMs are derived from parameterized
79 assumptions based on laboratory simulation and field observations. The actual
80 atmospheric chemical processes are very complex, and some reaction mechanisms are
81 still limitedly understood. In addition, the integration of chemical reactions and
82 simplified treatment methods in the model cannot fully reflect the correlation among
83 atmospheric pollutants. For example, in some model mechanisms, important sulfate and
84 nitrate formation pathways through new heterogeneous chemistry were added,
85 including the chemical reaction between SO₂ and aerosol, NO₂/NO₃/N₂O₃ and aerosol
86 (Zheng et al., 2015), nitrous acid oxidized SO₂ to produce sulfate (Zheng et al., 2020),
87 dust particles promoted the oxidation of SO₂ (Yu et al., 2020), modified the uptake
88 coefficients for heterogeneous oxidation of SO₂ to sulfate (Zhang et al., 2019), updated
89 the heterogeneous N₂O₅ parameterization (Foley et al., 2010). Even though the
90 aforementioned processes can significantly improve the simulation of SO₄²⁻ and NO₃⁻,
91 there is still a gap between the modeled and the actual atmospheric chemical processes.

92 The uncertainty of meteorological field simulation is another crucial reason for the
93 simulation deviation, especially on heavy pollution days, the variation trends of PM_{2.5}
94 chemical components were not well-captured (Ying et al., 2018; Qi et al., 2019; Wang
95 et al., 2022). Precipitation is the key meteorological factor determining wet removal of
96 pollutants; boundary layer height and wind speed are the main factors affecting
97 convection and transport of pollutants; solar radiation, temperature and relative
98 humidity are the key factors affecting the formation of secondary particles (Huang et
99 al., 2019; Chen et al., 2020). Some literature reported that deviation from precipitation
100 and wind field simulation might lead to underestimation of SO₄²⁻, NO₃⁻ and NH₄⁺
101 (Cheng et al., 2015; Zhang et al., 2017). Devaluation of liquid water path and cloud
102 cover cause a decrease of sulfate formation in cloud, and ultimately results in
103 significantly underestimated components in simulation values (Sha et al., 2019; Foley
104 et al., 2010). Underestimation of temperature and relative humidity may also cause
105 adverse effects of temperature- and/or relative humidity-dependence chemical reaction

106 in the simulation (Sha et al., 2019).

107 The uncertainty of source emission inventory also significantly affects the
108 simulation results of PM_{2.5} components (Shi et al., 2017; Sha et al., 2019). Due to
109 incomplete information or insufficient representativeness, pollutant emissions are
110 sometimes overestimated or underestimated, and the method for temporal and spatial
111 allocation also needs to be improved.

112 In particular, the emission source profile of PM_{2.5} (Hereinafter referred to as
113 "source profile"), used to create speciated emission inventories for CTMs (Hsu et al.,
114 2019), has not been fully taken into account in the current numerical simulation. In the
115 reported literatures, PM_{2.5} species allocation coefficients of emission sources are
116 commonly treated in the following ways: (1) allocated PM_{2.5} components of source
117 emissions by referring to source profile data in published literature or database like the
118 US SPECIATE (Fu et al., 2013; Wang et al., 2014; Ying et al., 2018); (2) chemical
119 profiles come from local measurement (Fu et al., 2013; Appel et al., 2013). However,
120 with the development of production technology and the innovation of pollution
121 treatment technology in recent years, some source profiles have changed dramatically
122 (Bi et al., 2019), such as SO₄²⁻ from coal burning, SO₄²⁻ content in PM_{2.5} is generally
123 low in coal-fired power plant without desulfurizing facilities, while existing coal-fired
124 power plants using limestone/gypsum wet desulphurization, the contents of SO₄²⁻ in
125 PM_{2.5} are significantly higher than that without desulfurization facilities (Zhang et al.,
126 2020). The timeliness of PM_{2.5} species allocation coefficients in current CTMs also
127 needs to be considered.

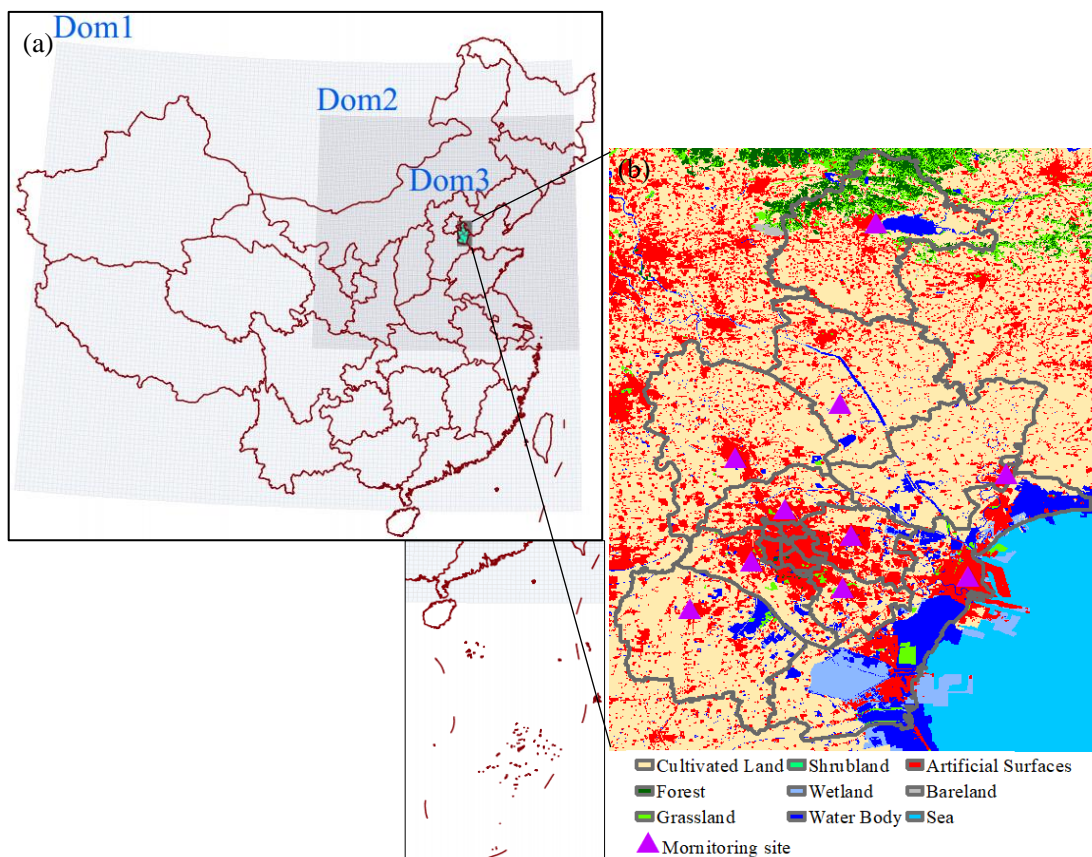
128 This paper attempts to answer the following questions: (1) Whether the variation
129 of the source profile adopted in the model has an impact on the simulated results of
130 PM_{2.5} chemical components? (2) How much does it impact? (3) How does the impact
131 work? Aiming at these problems above, chemical composition and its variation law for
132 typical PM_{2.5} emission sources are summarized, on this basis, sensitivity tests are
133 designed to identify whether PM_{2.5} source profiles and species allocation in the model
134 are important parameters that affect the simulation results of chemical components in

135 PM_{2.5}. We take CMAQ (one of the most widely used CTMs), MEIC (a high-resolution
136 inventory of anthropogenic air pollutants in China) as the carriers. The same kind of
137 experiment is also applicable to other CTMs and emission inventories. The aim of this
138 study is to provide support for the effective utilization of source profiles in the CTMs
139 and improvement of the simulation schemes.

140 **2. Model and Data**

141 **2.1 Model configuration**

142 Weather Research and Forecasting model (WRF-3.7.1), the widely used
143 Community Multiscale Air Quality model (CMAQv5.0.2), and Multi-resolution
144 Emission Inventory for China (MEICv1.3) have been used in this study. MEIC ,
145 developed by Tsinghua University, mainly tracked anthropogenic emissions in China
146 including coal-fired power plants, industry, vehicles, residents and agriculture
147 (http://meicmodel.org/?page_id=135) (Li et al., 2017b; Zheng et al., 2018). The WRF
148 model was used to generate meteorological inputs for the CMAQ model. Three nested
149 modeling domains consisting of 36 km×36 km (Dom1), 12 km×12km (Dom2), and 4
150 km×4km (Dom3) horizontal grid sizes were set, as shown in Fig. 1. The initial and
151 boundary conditions for WRF were based on the North American Regional Reanalysis
152 data archived at National Center for Atmospheric Research (NCAR). In addition,
153 surface and upper air observations obtained from NCAR were used to further refine the
154 analysis data. The modeling was conducted from Oct. 1 to Oct.30 in 2018, and major
155 configurations we used in CMAQ were illuminated as follows: Gas-phase chemistry
156 was based on the CB05 mechanism and the aerosol dynamics/chemistry was based on
157 the aero6 module (cb05tucl_ae6_aq). The detailed model configurations were shown in
158 Table S2, and regional distribution of PM_{2.5} emission sources were shown in Figure S1.



159
 160 Fig.1 Modeling domains of the CMAQ model. (a) The three-domain nested CMAQ domains; (b)
 161 Land use and observation sites of Dom3 (Data source of Land use: GLOBELAND30,
 162 www.globeland30.org, National Geomatics Center of China).

163 2.2 Selection and comparison of PM_{2.5} emission source profile

164 The PM_{2.5} emission source profiles from database of Source Profiles of Air
 165 Pollution (SPAP) (<http://www.nkspap.com:9091/>), U.S. Environmental Protection
 166 Agency's (EPA) SPECIATE database ([https://www.epa.gov/air-emissions-](https://www.epa.gov/air-emissions-modeling/speciate)
 167 modeling/speciate) as well as from published literature were selected, respectively. The
 168 SPAP was developed by the State Environment Protection Key Laboratory of Urban
 169 Particulate Air Pollution Prevention, Nankai University, China. This database contains
 170 more than 3000 size-resolved source profiles of stationary combustion sources,
 171 industrial processes, vehicle exhaust, biomass burning, dust and other sources, collected
 172 from more than 40 cities in China since 2001. In addition to inorganic elements, water-
 173 soluble ions, OC, EC and other conventional components, some source profiles also
 174 encompass a series of tracer information, such as organic markers, isotopes, single
 175 particle mass spectrometry, VOCs and other gaseous precursors. Based on species in

176 the aerosol chemical mechanism (AERO6) of CMAQ (Appel et al., 2013; Chapel Hill,
 177 2012), we selected 15 components in PM_{2.5} source profiles including Al, Ca, Cl, EC,
 178 Fe, K, Mg, Mn, Na, OC, Si, Ti, NH₄⁺, NO₃⁻ and SO₄²⁻, the remaining components are
 179 classified as “other”. In the database of Source Profiles of Air Pollution (SPAP) and
 180 U.S. Environmental Protection Agency’s (EPA) SPECIATE database, these four source
 181 categories (coal-fired power plant, industry process, transportation sector and
 182 residential coal combustion) contain a series of sub-categories. But the MEIC emission
 183 inventory does not include the corresponding sub-categories. So we take the average
 184 values of source profiles in each source category as representing source profile, the
 185 details could also be seen in our previous work (Bi et al., 2019); Then multiply
 186 inventory emissions by profile fraction to get emissions of specific chemical
 187 components.

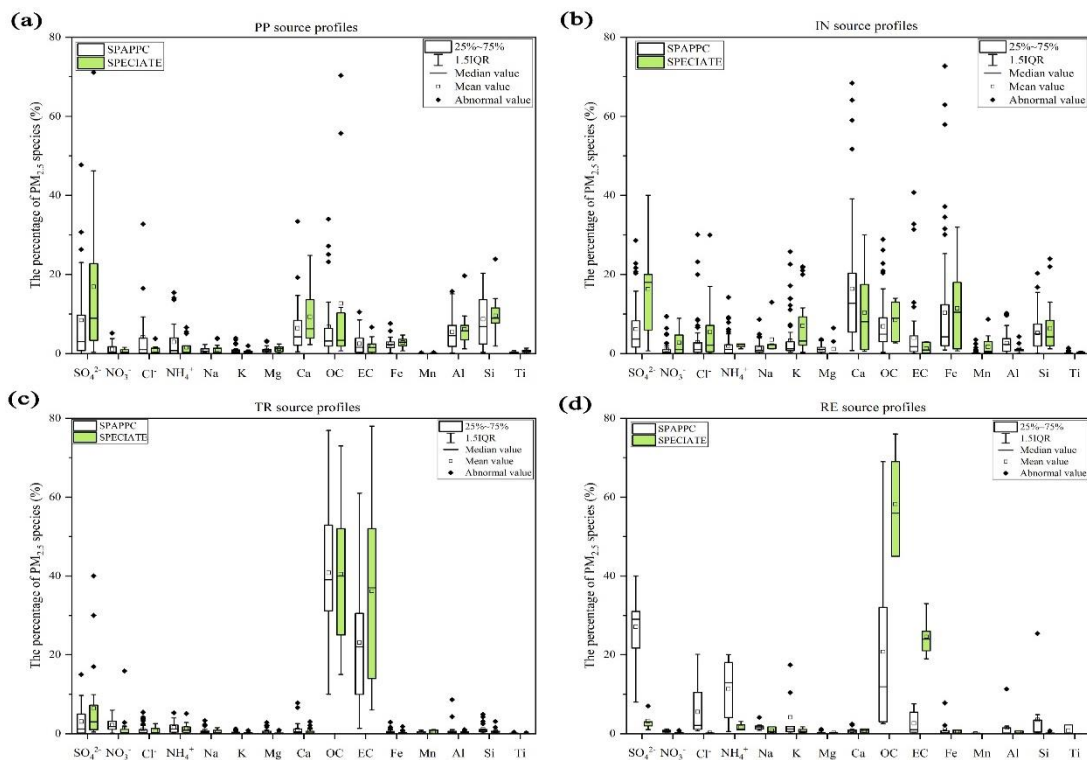
188 To determine the similarity between the two groups of source profiles, Coefficient
 189 Divergence (CD) is calculated using the following formula (Wongphatarakul et al.,
 190 1998):

$$191 \quad CD_{jk} = \sqrt{\frac{1}{p} \sum_{i=1}^p \left(\frac{x_{ij} - x_{ik}}{x_{ij} + x_{ik}} \right)^2} \dots\dots\dots (1)$$

192 Where CD_{jk} is the coefficient of divergence of source profile *j* and *k*, *p* is the
 193 number of chemical components in source profile, *x_{ij}* is the weight percentage for
 194 chemical component *i* in source profile *j*, *x_{ik}* is the weight percentage for *i* in source
 195 profile *k* (%). The CD value is in the range of 0 to 1, if the two source profiles are
 196 similar, the value of CD is close to 0; if the two are very different, the value is close to
 197 1.

198 **Coal-fired power plant (PP).** Coal-fired power plants remain the main coal
 199 consumers in China, which accounted for 50.2% of total coal consumption in 2019
 200 (NBS, 2021) and gained much more attention, especially with the wide implementation
 201 of the ultralow emission standards, PM_{2.5} emission characteristics have changed
 202 accordingly (Wu et al., 2020; Wu et al., 2022). There are obvious differences in PM_{2.5}
 203 source profiles between SPAPPC (SPAP database and published source profiles in

204 China) and SPECIATE (U.S.EPA SPECIATE database), the CD value of these two
 205 groups lie between 0.34 and 0.92 (0.64 ± 0.10), detailed information is shown in Table
 206 S3 and Figure S2. The percentages of species in PP source profiles are plotted in Fig.
 207 2(a). The main components in SPAPPC are sorted by Si, SO_4^{2-} , OC, Ca with average
 208 values of $8.7\pm 6.8\%$, $8.5\pm 11.5\%$, $6.8\pm 9.1\%$ and $6.5\pm 6.9\%$, respectively; The SPECIATE
 209 are enriched in SO_4^{2-} ($16.9\%\pm 20.0\%$), OC ($12.7\%\pm 21.8\%$), Si ($9.6\pm 5.0\%$) and Ca
 210 ($9.3\pm 7.3\%$), higher than SPAPPC. Coal properties, burning conditions, pollution control
 211 measures and emission sampling methods are the main reasons for those great
 212 percentage fluctuations. Different treatment processes of flue gases, e.g. wet/dry
 213 limestone, ammonia and double-alkali flue gas desulfurization, will affect the
 214 percentages of components in source profiles (Zhang et al., 2020). It has been reported
 215 that the percentage of Ca, Mg, SO_4^{2-} and Cl^- in PP profiles increased after the limestone-
 216 gypsum method was used in coal-fired power plants (Bi et al., 2019). Besides that, the
 217 percentage of Cl^- in SPAPPC is obviously higher than that in SPECIATE, which might
 218 attribute to the generally higher Cl^- content in raw coal in China (Guo et al., 2004).



219
 220 Fig. 2 Chemical profiles for $\text{PM}_{2.5}$ emitted from (a) coal-fired power plants (PP), (b) industry
 221 processes (IN), (c) transportation sector (TR), (d) residential coal combustion (RE). Data obtained

222 from SPAPPC (SPAP database and published source profiles in China) and SPECIATE (U.S. EPA
223 SPECIATE database)

224 **Industrial process(IN).** Industrial emissions are one of the major sources of PM_{2.5}
225 (Hopke et al., 2020), the percentages of Ca, Fe, OC and SO₄²⁻ are relatively high both
226 in SPAPPC and SPECIATE, but the shares in different source profile database varied,
227 their CD values vary from 0.45 to 0.94 (0.72±0.09) (Detailed information were shown
228 in Table S4~S7 and Figure S3). In SPAPPC, these four components account for
229 16.4±14.9%, 10.4±14.4%, 6.9±6.1%, 6.2±6.4%, the proportions in SPECIATE are
230 10.4±9.8%, 11.4±10.6%, 8.5±4.9%, 16.3±13.3%, respectively (Fig. 2(b)). Large
231 variations of components and their percentages in industrial processes are attributed to
232 the manufacturing processes, raw material, pollution control measures and so on (Ji et
233 al., 2017; Bi et al., 2019; Gao et al., 2022). For example, Ca, Al, OC and SO₄²⁻ are found
234 to have the highest percentage in cement sources (Guo et al., 2021); Fe, Si and SO₄²⁻
235 are the most abundant species in steel industry emission (Guo et al., 2017).

236 **Transportation sector (TR).** Traffic contributed a large fraction of PM_{2.5} in many
237 locations (Hopke et al., 2022). It is well-known that the transportation sector makes a
238 dominant contribution of OC and EC. The main components of PM_{2.5} emitted from
239 traffic sources are OC, EC and SO₄²⁻ both in SPAPPC and SPECIATE, but still vary in
240 wide range, their CD values fall between 0.33 and 0.86 (0.69±0.09) (Detailed
241 information was given in Table S8~S10 and Figure S4). In SPAPPC, the percentages of
242 OC, EC and SO₄²⁻ are 40.8±15.0%, 23.1±13.8%, 3.1±3.7%, and in SPECIATE, the
243 percentages are 40.6±16.4%, 36.1±21.5%, 6.4±9.9%, respectively (Fig. 2(c)). These
244 significant differences mainly attribute to the vehicle type, fuel quality, mixing ratio
245 between oil and gas and the combustion phase in vehicle engine and so on (Xia et al.,
246 2017).

247 **Residential coal combustion (RE).** Residential coal combustion, as the leading
248 source of global PM_{2.5} emission (Weagle et al., 2018), has a much higher emission
249 factor than coal-fired power plant (Wu et al., 2022). The fraction of components vary
250 greatly in the profiles measured from SPAPPC and SPECIATE, their CD values are
251 0.75±0.10 (Detailed information was given in Table S11 and Figure S5), SO₄²⁻, OC,

252 NH_4^+ and EC make the main contribution to $\text{PM}_{2.5}$ emitted from residential coal
253 combustion. In SPAPPC, the average percentages of SO_4^{2-} , OC, NH_4^+ , EC are
254 $27.1\pm 10.1\%$, $20.7\pm 20.6\%$, $11.3\pm 7.7\%$, $2.6\pm 2.8\%$, respectively. In SPECIATE, the
255 average percentages are OC ($58.2\pm 14.0\%$), EC ($24.6\pm 5.4\%$), SO_4^{2-} ($3.2\pm 2.3\%$) and
256 NH_4^+ ($1.6\pm 1.0\%$) (Fig. 2(d)). Total percentages of OC and EC in SPECIATE are over
257 80%, obviously higher than that in SPAPPC, while a higher percentage of SO_4^{2-} , Cl⁻, K
258 and Si are observed in SPAPPC. The coal type and properties, burning condition are the
259 main factors affecting the percentages of $\text{PM}_{2.5}$ components, like the chunk coal burning
260 has relatively higher percentages of OC, EC, SO_4^{2-} , NO_3^- and NH_4^+ than honeycomb
261 briquette (Wu et al., 2021; Song et al., 2021).

262 Briefly, many factors can affect $\text{PM}_{2.5}$ source profiles, and with the innovation of
263 manufacturing technique and pollution control technology, changes in fuel and raw and
264 auxiliary materials, the main chemical components and their percentages would change
265 dramatically. To explore whether the variations of source profile adopted in CMAQ
266 model would be one of the important factors affecting the simulated $\text{PM}_{2.5}$ component,
267 we designed a series of simulation tests to address the following issues.

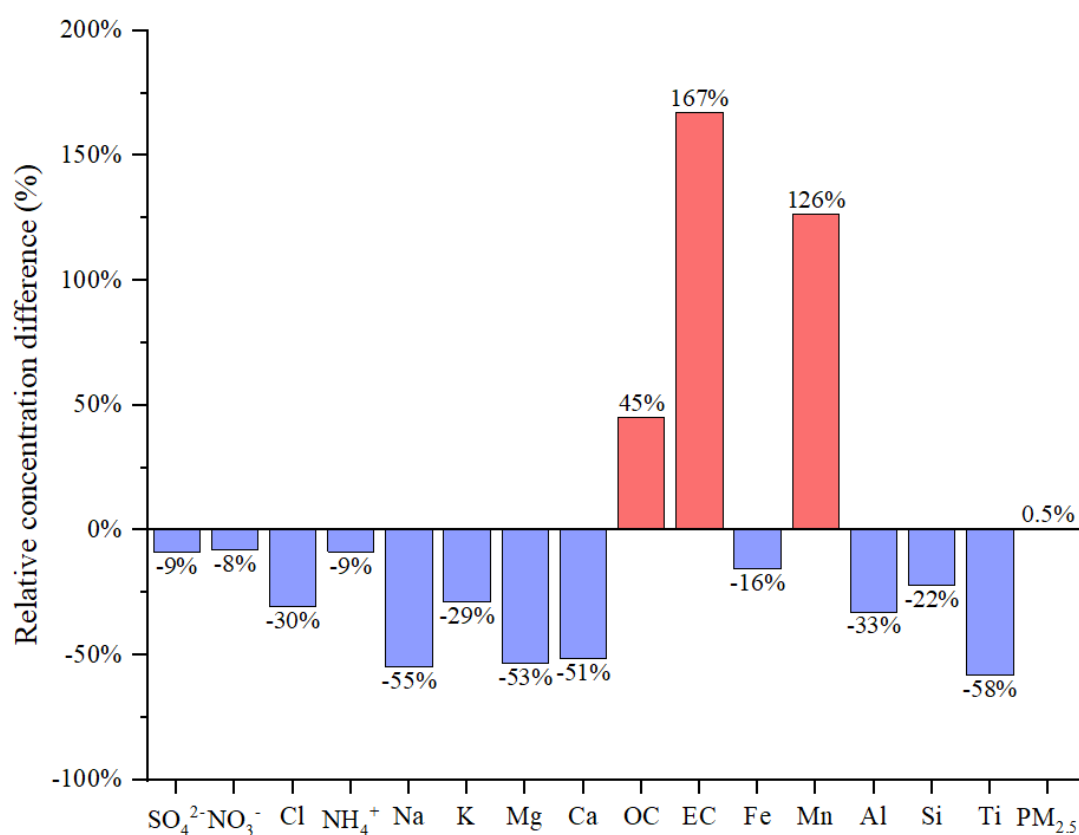
268 **3 Is there an impact of variation of source profile on the simulation results?**

269 In this part, we separately selected source profiles from SPAPPC and SPECIATE
270 databases and applied them in emission inventory for simulating $\text{PM}_{2.5}$ and its
271 components with other modeling conditions unchanged, corresponding to case
272 CMAQ_SPA and CMAQ_SPE. The detailed information of source profiles is shown in
273 Figure S6.

274 By comparing the selected SPAPPC source profiles with the selected SPECIATE
275 source profiles, the coefficient divergences for the four main source categories were
276 $\text{CD}_{\text{PP}}(0.67) > \text{CD}_{\text{RE}}(0.62) > \text{CD}_{\text{TR}}(0.60) > \text{CD}_{\text{IN}}(0.60)$, which meant the selected source
277 profiles in the two simulation cases were quite different. The average simulated
278 concentration of $\text{PM}_{2.5}$ and its components at each ambient air quality monitoring
279 station (Table S12) were extracted from CMAQ outputs. We selected one air quality

280 monitoring station (Site 8 as the selected station here and any site could be available)
 281 to explore the effect of emission source chemical profiles on simulated PM_{2.5}
 282 components, then used the left 9 sites to further illustrate the conclusions suggested.

283 The simulation results for PM_{2.5} species under CMAQ_SPA and CMAQ_SPE
 284 cases also showed big differences (as shown in Fig. 3 and Table S13). The largest
 285 difference in average simulated concentration was EC with CAMQ_SPE giving higher
 286 by 167% than CMAQ_SPA; For OC and Mn, higher values were also given by
 287 CMAQ_SPE than by CMAQ_SPA (45% and 126% on average, respectively); For the
 288 other components of concern, the simulated concentration by CMAQ_SPE was lower
 289 than CMAQ_SPA with Ti (58%), Na (55%), Mg (53%), Ca (51%), Al (33%), Cl (30%),
 290 K (29%), Si (22%), Fe (16%), NH₄⁺ (9%), SO₄²⁻ (9%), NO₃⁻ (8%), separately. While the
 291 simulated PM_{2.5} concentrations under the two cases were quite close. The influence of
 292 source profile variation on the simulated PM_{2.5} concentration was not significant, but
 293 the influence on the simulation of chemical components in PM_{2.5} could not be ignored.



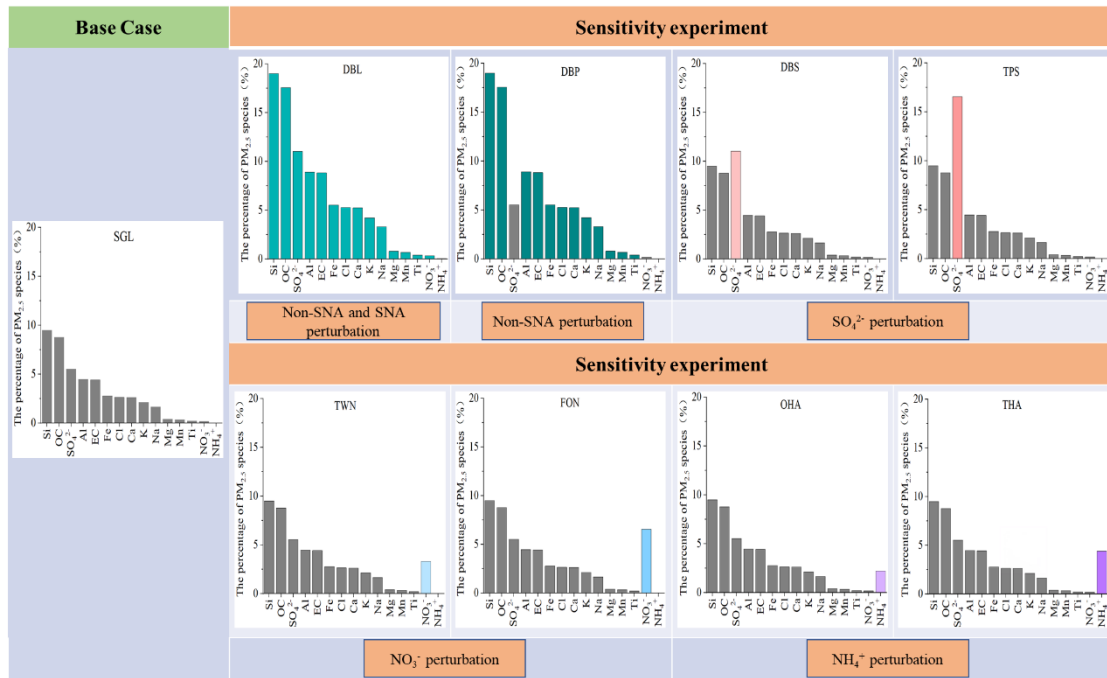
294

295 Fig. 3 The relative concentration difference of average simulated result (PM_{2.5} and its components)

296 between CMAQ_SPE and CAMQ_SPA (relative to CAMQ_SPA) during simulation period; PM_{2.5}
 297 source profiles from SPAPPC and SPECIATE database were used to create speciated emission
 298 inventories for CMAQ, corresponding to case CMAQ_SPA and CMAQ_SPE, respectively.

299 **4 How much does it impact?**

300 To quantitatively characterize how much the source profiles affect the simulation
 301 results, we selected the chemical composition of code 000002.5 (Variety of different
 302 categories, used for the overall average composite profiles (Hsu et al., 2019)) in the US
 303 EPA Speciate_5.0_0 database for species allocation of PM_{2.5} components. The
 304 corresponding percentages of EC, OC, Mn, Fe, Ti, Al, Si, Ca, Mg, K, Na, Cl, NH₄⁺,
 305 NO₃⁻ and SO₄²⁻ in PM_{2.5} were shown in Fig. 4 (SGL, base case simulation).



306
 307 Fig. 4 The general roadmap of sensitivity tests (The histogram in each case were the speciation
 308 profile in CTMs; SNA represent SO₄²⁻, NO₃⁻, and NH₄⁺, Non-SNA represent other components in
 309 PM_{2.5}).

310 Table 1 The content of sensitivity experiment cases

Experiment Cases	Description ³
Case DBL: add perturbation to Non-SNA and SNA ¹	The percentage of all the listed components in the source profile of base case (SGL) were doubled, and the proportion of unlisted components (Other) ² decreased to 9%.
Case DBP:	The percentages of non-SNA were doubled and SNA(SO ₄ ²⁻ ,

add perturbation to Non-SNA	NO ₃ ⁻ , NH ₄ ⁺) species stayed the same with that in SGL (the cumulative percentage of listed species was 85.3%), the proportion of unlisted components decreased to 14.7%.
Case DBS and TPS: add perturbation to SO ₄ ²⁻	The percentage of SO ₄ ²⁻ was doubled (11%, DBS, represented Double Sulfate), tripled (16.5%, TPS, represented Triple Sulfate) and the other listed 14 species stayed the same with that in SGL (the cumulative percentage of listed species was 51% and 57%, respectively), the proportion of unlisted components decreased to 49% and 43%.
Case TWN and FON: add perturbation to NO ₃ ⁻	The NO ₃ ⁻ content was raised up to 20 times (3.3%, TWN) and 40 times (6.6%, FON) of that in SGL (0.16%), the other 14 species stayed the same with SGL (the cumulative percentage of listed species was 48.6% and 51.9%, respectively), the proportion of unlisted components decreased to 51.4% and 48.1%.
Case OHA and THA: add perturbation to NH ₄ ⁺	The NH ₄ ⁺ content was raised up to 100 times (2.2%, OHA), 200 times (4.4%, THA) of that in SGL (0.02%), the other 14 species stayed the same with SGL (the cumulative percentage of listed species was 47.7% and 49.9%, respectively), the proportion of unlisted components decreased to 52.3% and 50.1%.

Note:

1. SNA represent SO₄²⁻, NO₃⁻, and NH₄⁺, Non-SNA represent other components in PM_{2.5}.
2. The listed components contain Al, Ca, Cl, EC, Fe, K, Mg, Mn, Na, OC, Si, Ti, NH₄⁺, NO₃⁻ and SO₄²⁻, unlisted components are classified as Other.
3. The source profiles in all cases listed in the table were calculated based on the base case SGL. In the design of simulation cases, the reason why the disturbance amplitude of NH₄⁺ and NO₃⁻ were significantly higher than that of other components such as SO₄²⁻ and Non-SNA, was because the percentages of NH₄⁺ and NO₃⁻ in the base source profile (SGL, based on the chemical composition of code 000002.5 in the EPA Speciate_5.0_0 database) were very low, while the percentage of NH₄⁺ and NO₃⁻ in SPAPPC exhibited in section 2.2 were orders of magnitude higher than those in SGL.

311 Given the large number and complex chemical composition of PM_{2.5}, it is
312 advisable to classify them reasonably before designing sensitivity experiments. The
313 Case DBL was to double the percentage of the listed 15 components mentioned in the
314 above base case(SGL) (the details are shown in Fig. 4 and Table 1). As the percentage
315 of these components increased, the proportion of unlisted components (represented by
316 “Other”) decreased to 9% in order to meet the requirement that the total percentage of
317 all components is 100%. Then we compared the simulation results before (SGL case)

318 and after perturbation (DBL case) in species allocation of PM_{2.5} sources.

319 In the case DBL, when the percentage of all the components except “other” were
320 doubled in the source profile, the simulated concentrations of Al, Ca, Cl, EC, Fe, K,
321 Mg, Mn, Na, OC, Si and Ti doubled as well, while the simulated concentration of NO₃
322 and SO₄²⁻ increased at about 3%, 10% and NH₄⁺ decreased by 4%, respectively,
323 although the simulated concentration of PM_{2.5} was not obviously changed (Detailed
324 simulation results were shown in Table S14). The simulation test results for SNA (SO₄²⁻,
325 NO₃⁻, and NH₄⁺) and Non-SNA were obviously different. Therefore, we divided the
326 components in the source profile into two groups (Non-SNA and SNA) and designed a
327 series of sensitivity tests listed in next section to further explore how species allocation
328 of PM_{2.5} in emission sources affect the simulation results. The sketch of sensitivity
329 experiment design idea is shown in Figure S7.

330 4.1 Sensitivity tests design

331 Sensitivity tests were designed by changing the percentages of the target
332 components and related components in the base case (SGL): add perturbation on each
333 component of Non-SNA, on SO₄²⁻, on NO₃⁻, and on NH₄⁺. The general roadmap of
334 sensitivity tests is shown in Fig. 4, and the illustration of each case was summarized in
335 Table 1. The basic rules must be followed: a) perturbation on the percentage of each
336 component in source profile fell within the variation range of its measured value
337 described in section 2.2. b) The sum of the percentage of listed Non-SNA, SNA and
338 Other components in PM_{2.5} source profile was 100%.

339 4.2 Sensitivity of simulated components to changes in source profile

340 We proposed the sensitivity coefficient (δ) as evaluation index. The calculation
341 formula is as follows:

$$342 \delta_{i,p} = \frac{\frac{C_{i_case}}{C_{PM_{2.5_case}}} \times 100\% - \frac{C_{i_base}}{C_{PM_{2.5_base}}} \times 100\%}{P_{p_case} - P_{p_base}} \quad (\text{For DBL and DBP, } p = i; \text{For other cases, } p = j)$$

343 (2)

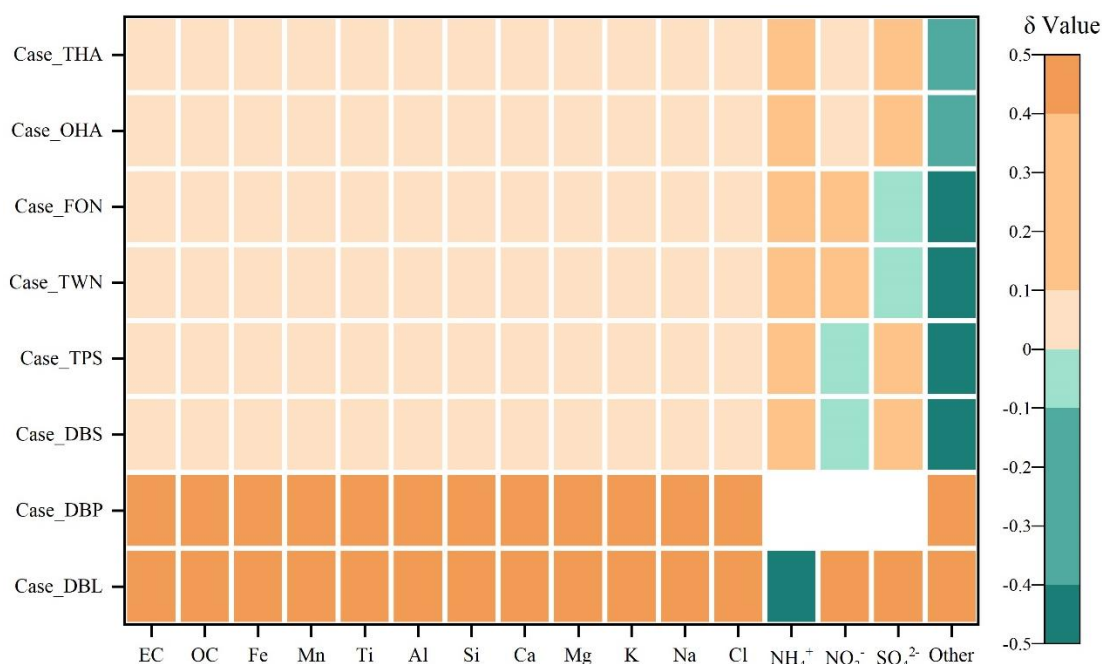
344 Wherein, δ_{i,p} is the sensitivity coefficient of component *i* relative to component *p*,

345 representing the change in simulated value of its content in ambient PM_{2.5} corresponded
346 to 1% perturbation in the source profiles. C_{i_case} is the simulation result of component I
347 in each sensitivity experiment case, $\mu\text{g}/\text{m}^3$; C_{i_base} is the simulation result of components
348 i in base case, $\mu\text{g}/\text{m}^3$; $C_{PM_{2.5_case}}$ is the simulation result of PM_{2.5} in each sensitivity
349 experiment case, $\mu\text{g}/\text{m}^3$; $C_{PM_{2.5_base}}$ is the simulation result of PM_{2.5} in base case, $\mu\text{g}/\text{m}^3$;
350 P_{p_case} is the percentage of component p in source profile of sensitivity experiment
351 case, %; j is the perturbed component j in different source profile of sensitivity
352 experiment cases; P_{p_base} is the percentage of component p in source profile of base
353 case, %.

354 The positive value of δ means the simulated concentration of PM_{2.5} component
355 increases (decreases) with the increase (decrease) of perturbation on the percentage of
356 components in source profile, negative δ is just the opposite. If the absolute value of δ
357 is less than or equal to 0.1, the simulated component is considered to be insensitive to
358 the corresponding variation of source profile; If the absolute value of δ falls between
359 0.1 and 0.4 (included), the simulated component is considered to be sensitive to the
360 variation of source profile; If the absolute value of δ is larger than 0.4, the simulated
361 component is very sensitive to the variation of source profile. The greater the absolute
362 value of δ is, indicates the variation of source profile adopted in CMAQ has more
363 obvious impact on the simulated results of PM_{2.5} chemical components.

364 Fig.5 listed the sensitivity coefficients of simulated ambient PM_{2.5} components to
365 the perturbation of source profile under each test case. In case DBL (doubled the
366 percentage of the listed components in the source profile of base case and decreased the
367 proportion of unlisted other components to 9%), , the sensitivity coefficient (δ) of NH_4^+
368 was negative, and the absolute value was high, indicating that the simulated proportion
369 of NH_4^+ in ambient PM_{2.5} decreased, and it was very sensitive to the variation of source
370 profile. Conversely, the sensitivity coefficient of NO_3^- was close to 1, which illustrated
371 that the simulated proportion of NO_3^- in ambient PM_{2.5} increased proportionally with
372 the change in source profile. The simulated SO_4^{2-} also showed a very sensitive property.

373 The simulated Non-SNA concentrations were doubled when compared to the base case
 374 (SGL).



375
 376 Fig. 5 The sensitivity coefficients (δ) of simulated components to the perturbation of adopted source
 377 profile in different cases. Note: Each small color box in the figure represented the sensitivity level
 378 (indicated by the legend on the right) of PM_{2.5} components (the x-coordinate) in different cases (y-
 379 coordinate). The blank grids in DBP case indicated no perturbation to SNA in PM_{2.5} source profile
 380 under this case.

381 In case DBP, when the percentages of listed Non-SNA (Al, Ca, Cl, EC, Fe, K, Mg,
 382 Mn, Na, OC, Si and Ti) in the source profile were doubled, the simulated proportions
 383 of Non-SNA in ambient PM_{2.5} synchronous increased, and were very sensitive to the
 384 change in the adopted source profile with a sensitivity coefficient (δ) of 0.5.
 385 Interestingly, the simulated concentration of SNA in ambient PM_{2.5} also changed
 386 although the SNA in source profile did not change, the concentration of NO₃⁻ and SO₄²⁻
 387 increased by 2% and 3%, respectively, NH₄⁺ decreased by 10% (Detail simulation
 388 results of each case were shown on Table S15~S21).

389 Under SO₄²⁻ perturbation cases (Case DBS and Case TPS), we found the simulated
 390 results of Non-SNA and NO₃⁻ had no obvious variation compared with the base case.
 391 Either in Case DBS or in Case TPS, the δ of Non-SNA and NO₃⁻ were between -0.1 to
 392 0.1. But when the percentage of SO₄²⁻ was doubled in source profile (DBS), the

393 simulated concentration of NH_4^+ and SO_4^{2-} increased by 6% and 8%, respectively. In
394 Case TPS (the percentage of SO_4^{2-} was tripled), the simulated concentration of NH_4^+
395 and SO_4^{2-} were increased by 11% and 16%, respectively. The δ of NH_4^+ and SO_4^{2-} were
396 0.12 and 0.36, sensitive toward to positive direction with the increase of SO_4^{2-} in the
397 source profile.

398 In the situation of NO_3^- perturbation in source profile (Case TWN and Case FON),
399 the simulated Non-SNA hardly change when compared to the base case, while changing
400 patterns of simulated SNA were different. The simulation concentration of NH_4^+
401 increased by 2.6% and 5.4% compared with the base case, the simulated NO_3^- increased
402 by 14% and 30%, the simulated SO_4^{2-} decreased slightly, even could be neglected in
403 some observation sites. The simulated concentrations of Non-SNA and SO_4^{2-} were
404 insensitive to the perturbation of NO_3^- in source profile; NH_4^+ was sensitive, and NO_3^-
405 was very sensitive.

406 When we put perturbation on NH_4^+ in the source profile (Case OHA and Case
407 THA), the simulation results of Non-SNA were almost not changed, the simulated
408 concentration of SO_4^{2-} , NH_4^+ , NO_3^- increased. The δ of SNA to the variation of NH_4^+ in
409 the source profile were positive and $\delta_{\text{SO}_4^{2-}, \text{NH}_4^+} > \delta_{\text{NH}_4^+, \text{NH}_4^+} > \delta_{\text{NO}_3^-, \text{NH}_4^+}$, SO_4^{2-} and NH_4^+
410 were sensitive to the NH_4^+ perturbation in the source profile, but NO_3^- was not so
411 sensitive.

412 In general, the simulation results of components in ambient $\text{PM}_{2.5}$ were affected in
413 one way or another by the change of source profiles adopted by CMAQ. Both of the
414 simulated Non-SNA and SNA were very sensitive to the perturbation of Non-SNA in
415 source profile. When the percentage of SNA changed in the source profile, simulated
416 Non-SNA generally have little change, but the simulation results of SNA could change
417 in different patterns: the simulated SO_4^{2-} was very sensitive and NH_4^+ was sensitive to
418 the perturbation of SO_4^{2-} in source profile; simulated NO_3^- was very sensitive and NH_4^+
419 was sensitive to the perturbation of NO_3^- in source profile; SO_4^{2-} and NH_4^+ were
420 sensitive to the perturbation of NH_4^+ in source profile. The simulated component such
421 as SO_4^{2-} was influenced not only by the change of SO_4^{2-} itself but also by other

422 components like some Non-SNA and NH_4^+ in the source profile. In other words, there
 423 was a linkage effect, variation of some components in the source profile would bring
 424 changes to the simulated results of other components.

425 **5 How does the impact work?**

426 The variation of species allocation in emission sources can directly affect the
 427 composition of aerosol system in CTMs. In CMAQv5.0.2, the aerosol thermodynamic
 428 equilibrium process is carried out according to ISORROPIA II, including a SO_4^{2-} - NO_3^- -
 429 Cl^- - NH_4^+ - Na^+ - K^+ - Mg^{2+} - Ca^{2+} - H_2O system (Detailed equilibrium relations were shown
 430 in Table S22). Some assumptions had been made in the ISORROPIA model to simplify
 431 the simulation system (Fountoukis and Nenes, 2007): (1) Because the vapor pressure
 432 of sulfuric acid and metal salts (such as Na^+ , Ca^{2+} , K^+ , Mg^{2+}) were very low, it was
 433 assumed that all the sulfuric acid and metal salts in the system existed in the aerosol
 434 phase; (2) For ammonia in the system, it was preferred to have an irreversible reaction
 435 with sulfuric acid to produce ammonium sulfate. Only when there was still surplus NH_3
 436 after the neutralization of H_2SO_4 , can it have a reversible reaction with HNO_3 and HCl
 437 to produce NH_4NO_3 and NH_4Cl . (3) For sulfuric acid in the system, if there were metal
 438 ions (such as Ca^{2+} , Mg^{2+} , K^+ , Na^+) in the system, sulfuric acid would react with metal
 439 ions to produce metal salts. Only in the case of insufficient sodium, sulfuric acid would
 440 react with ammonia. Based on these assumptions, the ISORROPIA model introduced
 441 the following three judgment parameters (R_1 , R_2 and R_3) to determine the simulation
 442 subsystems, these parameters are calculated by the following formulas:

443
$$R_1 = \frac{[\text{NH}_4^+] + [\text{Ca}^{2+}] + [\text{K}^+] + [\text{Mg}^{2+}] + [\text{Na}^+]}{[\text{SO}_4^{2-}]} \dots\dots\dots (3)$$

444
$$R_2 = \frac{[\text{Ca}^{2+}] + [\text{K}^+] + [\text{Mg}^{2+}] + [\text{Na}^+]}{[\text{SO}_4^{2-}]} \dots\dots\dots (4)$$

445
$$R_3 = \frac{[\text{Ca}^{2+}] + [\text{K}^+] + [\text{Mg}^{2+}]}{[\text{SO}_4^{2-}]} \dots\dots\dots (5)$$

446 Where $[X]$ denotes molar concentration of component ($\text{mol}\cdot\text{m}^{-3}$), R_1 , R_2 and R_3

447 are termed as “total sulfate ratio”, “crustal species and sodium ratio” and “crustal
 448 species ratio” respectively; The number of species and equilibrium reactions are
 449 determined by the relative abundance of NH₃, Na, Ca, K, Mg, HNO₃, HCl, H₂SO₄, as
 450 well as the ambient relative humidity and temperature. Guided by the value of R₁, R₂
 451 and R₃, 5 aerosol composition regimes in ISORROPIA are defined. (Detail rules are
 452 shown in Table S27).

453 In this paper, R₁, R₂, R₃ and the potential aerosol species under each sensitivity
 454 test case were shown in Table 2. These components achieved thermodynamic
 455 equilibrium in the order of preference for more stable salts, obviously, the simulation
 456 processes of these components may influence each other.

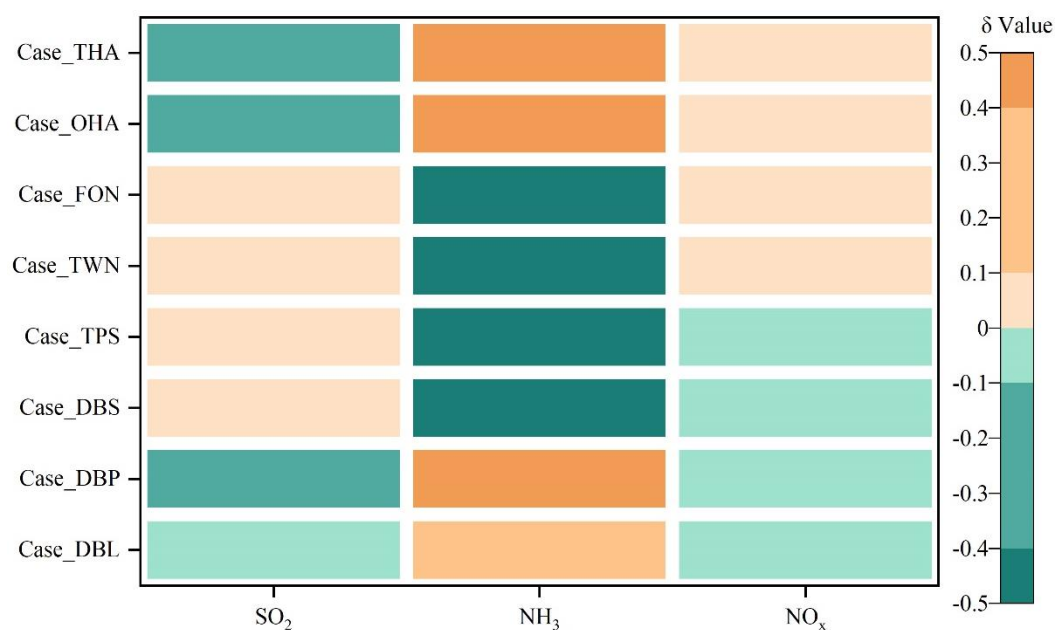
457 Table 2 Potential aerosol species in ISORROPIA II under different cases

Cases	R ₁	R ₂	R ₃	Solid phase species*
SGL	2.53	2.52	1.9	CaSO ₄ , MgSO ₄ , K ₂ SO ₄ , Na ₂ SO ₄ , NaCl, NaNO ₃ , NH ₄ Cl, NH ₄ NO ₃
DBL	2.53	2.52	1.9	CaSO ₄ , MgSO ₄ , K ₂ SO ₄ , Na ₂ SO ₄ , NaCl, NaNO ₃ , NH ₄ Cl, NH ₄ NO ₃
DBP	5.04	5.03	3.79	CaSO ₄ , MgSO ₄ , K ₂ SO ₄ , CaCl ₂ , Ca(NO ₃) ₂ , MgCl ₂ , Mg(NO ₃) ₂ , KCl, KNO ₃ , NaCl, NaNO ₃ , NH ₄ Cl, NH ₄ NO ₃
DBS	1.26	1.26	0.95	CaSO ₄ , MgSO ₄ , K ₂ SO ₄ , KHSO ₄ , Na ₂ SO ₄ , NaHSO ₄ , (NH ₄) ₂ SO ₄ , NH ₄ HSO ₄ , (NH ₄) ₃ H(SO ₄) ₂
TPS	0.84	0.84	0.63	CaSO ₄ , KHSO ₄ , NaHSO ₄ , NH ₄ HSO ₄
TWN	2.53	2.52	1.9	CaSO ₄ , MgSO ₄ , K ₂ SO ₄ , Na ₂ SO ₄ , NaCl, NaNO ₃ , NH ₄ Cl, NH ₄ NO ₃
FON	2.53	2.52	1.9	CaSO ₄ , MgSO ₄ , K ₂ SO ₄ , Na ₂ SO ₄ , NaCl, NaNO ₃ , NH ₄ Cl, NH ₄ NO ₃
OHA	3.58	2.52	2.95	CaSO ₄ , MgSO ₄ , K ₂ SO ₄ , CaCl ₂ , Ca(NO ₃) ₂ , MgCl ₂ , Mg(NO ₃) ₂ , KCl, KNO ₃ , NaCl, NaNO ₃ , NH ₄ Cl, NH ₄ NO ₃
THA	4.64	2.52	4.02	CaSO ₄ , MgSO ₄ , K ₂ SO ₄ , CaCl ₂ , Ca(NO ₃) ₂ , MgCl ₂ , Mg(NO ₃) ₂ , KCl, KNO ₃ , NaCl, NaNO ₃ , NH ₄ Cl, NH ₄ NO ₃

458 * The solid phase species were determined based on the research of (Fountoukis and Nenes, 2007)

459 In Non-SNA perturbation case, when the percentage of Non-SNA in source profile
 460 doubled (Case DBP), meant there were more Na, K, Mg, Ca, Cl participated in aerosol

461 chemistry, the model system needed more SO_4^{2-} and NO_3^- on the basis of charge balance
 462 and the thermodynamic equilibrium shifted to the direction of consuming Ca Mg, K
 463 and Na, which resulted in the increase of the simulated concentration of SO_4^{2-} and NO_3^- .
 464 Meanwhile, according to the rule of anions preferentially binding with nonvolatile
 465 cations in ISORROPIA, the increased cations Na^+ , K^+ , Mg^{2+} , Ca^{2+} directly led to
 466 the decrease of anions binding with NH_4^+ , there were less reaction dose between SO_4^{2-}
 467 and NH_4^+ to form $(\text{NH}_4)_2\text{SO}_4$ or NH_4HSO_4 , ultimately resulted in a decrease in
 468 simulated concentration of NH_4^+ compared with the base case. Because in this case
 469 more anions such as SO_4^{2-} were passively needed, according to the principle of chemical
 470 equilibrium mentioned above, the chemical conversion of SO_2 to SO_4^{2-} was promoted,
 471 the simulated secondary SO_4^{2-} increased, this could be proved by that the sensitivity
 472 coefficient δ of SO_2 in Case DBP was negative (shown in Fig. 6, details of other
 473 monitoring stations were shown Table S24).



474
 475 Fig.6 The sensitivity coefficients (δ) of simulated gas pollutants to the change of adopted source
 476 profile in different cases.

477 Similarly, with the increase of metal ions in the system to bond with anions, the
 478 number of anions which can bind to NH_4^+ decreased. The system needed less NH_4^+ and
 479 weakened the need for conversion from NH_3 to NH_4^+ , the simulated NH_4^+ concentration
 480 decreased while the δ of NH_3 was positive and very sensitive. Different trends of

481 simulated concentration of gaseous pollutants mirrored the rules mentioned above from
482 another aspect. The δ of SO_2 and NO_x was negative, NH_3 was positive. We could see
483 the same phenomena in DBL case (Fig. 6). When the percentages of Non-SNA in source
484 profile increased, they not only affected the simulated concentration of Non-SNA, but
485 also the secondary SO_4^{2-} , NO_3^- and NH_4^+ .

486 In SO_4^{2-} perturbation cases (Case DBS and TPS), as the percentage of SO_4^{2-} in
487 source profile increased, for the chemical reactions of sulfate radical consuming (as
488 shown in Table S22), the chemical equilibrium would move toward the products
489 compared with the base case. While for the chemical reactions of sulfate radical
490 formation (The equations were shown in Table S23), meant the product was added in,
491 the chemical equilibrium would be pushed toward the reactants. The chemical reactions
492 between SO_4^{2-} and NH_4^+ would shift to the direction of $(\text{NH}_4)_2\text{SO}_4$ generation, we could
493 see the simulated concentrations of NH_4^+ in DBS and TPS were both higher and NH_3
494 were lower than those in the base case (SGL). In addition, when more SO_4^{2-} was added
495 in the system, the conversion of SO_2 to SO_4^{2-} was affected in some level and consumed
496 less SO_2 than the base case, simulated SO_2 showed insensitive but positive trend (Fig.9).
497 And the potential solid phase species in ISORROPIA II under DBS and TPS cases
498 (shown in Table 2) were mainly consisted of sulfate salts, so the simulated concentration
499 of NO_3^- did not change apparently.

500 As the percentage of NO_3^- in source profile increased (Case FON and TWN), the
501 associated chemical equilibrium shifted towards the consumption of NO_3^- , such as NH_4^+
502 + $\text{NO}_3^- \rightarrow \text{NH}_4\text{NO}_3$, which would also consume more NH_4^+ and form more ammonium
503 salt, finally consumed more NH_3 because of $\text{NH}_3(\text{gas}) + \text{H}_2\text{O}(\text{aq}) \rightarrow \text{NH}_4^+(\text{aq}) + \text{OH}^-$
504 (aq). The simulation results also manifested that the concentration of NH_4^+ increased
505 while that of NH_3 decreased. Based on the assumption of ISORROPIA, the cations like
506 Na^+ , K^+ , Mg^{2+} , Ca^{2+} and NH_4^+ preferentially to react with SO_4^{2-} , only if there were
507 cations left after neutralized SO_4^{2-} , could they react with NO_3^- to form salts, so the
508 simulated concentration of SO_4^{2-} was not obviously changed. Accordingly, the
509 simulated concentration of NO_x and SO_2 almost unchanged (The δ of NO_x and SO_2

510 displayed insensitive).

511 In the cases of NH_4^+ perturbation (Case OHA and THA), when the percentage of
512 NH_4^+ in source profile increased, the related chemical equilibrium shifted towards the
513 direction of NH_4^+ consumption, such as in $2\text{NH}_4^+ + \text{SO}_4^{2-} \rightarrow (\text{NH}_4)_2\text{SO}_4$, more SO_4^{2-}
514 was consumed at the same time, which further promoted the conversion of SO_2 to SO_4^{2-} .
515 The increased NH_4^+ in OHA and THA also would inhibit the conversion of NH_3 to NH_4^+
516 compared with the base case. This, in turn appeared as the increase of the simulated
517 secondary SO_4^{2-} and NH_3 , and the decrease of the simulated SO_2 .

518 In summary, the effects of source profile variation on the simulation results of
519 different components were linked. When the percentages of Non-SNA, SO_4^{2-} , NO_3^- and
520 NH_4^+ in the source profile changed, they not only affected the simulated concentration
521 of themselves, but also affected the simulation results of some other components. Both
522 the simulation results of primary components and secondary components were affected
523 by the change of source profile, the secondary SO_4^{2-} and NH_4^+ were affected more than
524 the secondary NO_3^- .

525 **6 Conclusions**

526 The influence of source profile variation on the simulated $\text{PM}_{2.5}$ components
527 cannot be ignored, as simulation results of some components are sensitive to the
528 adopted source profile in CTMs, e.g., both the simulated Non-SNA and SNA are
529 sensitive to the perturbation of Non-SNA in source profile, the simulated SO_4^{2-} and
530 NH_4^+ are sensitive to the perturbation of SO_4^{2-} , simulated NO_3^- and NH_4^+ are sensitive
531 to the perturbation of NO_3^- , SO_4^{2-} and NH_4^+ are sensitive to the perturbation of NH_4^+ .
532 These influences are not only specific to an individual component, but also can be
533 transmitted and linked among components. The influence path is connected to chemical
534 mechanisms in the model since the variation of species allocation in emission sources
535 directly affect the thermodynamic equilibrium system (ISORROPIA II, SO_4^{2-} - NO_3^- - Cl^-
536 - NH_4^+ - Na^+ - K^+ - Mg^{2+} - Ca^{2+} - H_2O system).

537 It is generally believed that changes in source profile would have an impact on the

538 simulation result of primary PM_{2.5}, but interestingly, the simulation of secondary
539 components could be affected as well. We found the perturbation of PM_{2.5} source profile
540 caused the variation of simulation results of gaseous pollutants by influencing related
541 chemical reactions like gas-phase chemistry of SO₂, NO_x and NH₃. Overall, the
542 emission source profile used in CTMs is one of the important factors affecting the
543 simulation results of PM_{2.5} chemical components. Additionally, organic species are one
544 of the most important components in PM_{2.5} and gain much more attention on human
545 health. While the number of organic species in source profile is relatively scarce which
546 brings a challenge for simulation test designing, the influence of source profile on the
547 simulation results of organic species is not taken into account in this study.

548 With the change of fuel and raw materials, the development of production
549 technology and the innovation of pollution treatment technology in recent years, some
550 components have changed significantly in source profiles. Given the important role of
551 air quality simulation in decision making for pollution control and health risk
552 assessment, the representativeness and timeliness of the source profile should be
553 considered.

554 Our study tentatively discussed the influence mechanism of PM_{2.5} emission source
555 profiles on the simulation results of components in CTMs. The size distribution, mixing
556 state, aging and solubility for different aerosol components might have something to do
557 with source profile, how much the influence of source profile changes on the simulation
558 of these physical and chemical process, is deserved to do in the future.

559 **Data availability**

560 The input datasets for WRF simulation are available at
561 <https://rda.ucar.edu/datasets/ds351.0/index.html> (The National Center for Atmospheric
562 Research (NCAR)). The Multi-resolution Emission Inventory for China (MEICv1.3) is
563 available at http://meicmodel.org/?page_id=135. The PM_{2.5} emission source profiles
564 from database of Source Profiles of Air Pollution (SPAP)
565 (<http://www.nkspap.com:9091/>, Nankai university), SPECIATE database

566 (<https://www.epa.gov/air-emissions-modeling/speciate>, U.S. Environmental Protection
567 Agency's (EPA)), Mendeley data repository (<https://doi.org/10.17632/x8dfshjt9j.2>, Bi
568 et al., 2019).

569 **Code availability**

570 The source code for CMAQ version 5.0.2 is available at
571 <https://github.com/USEPA/CMAQ/tree/5.0.2> (last access: April 2014)
572 (<https://doi.org/10.5281/zenodo.1079898>, US EPA Office of Research and
573 Development, 2018). The source code for WRF version 3.7.1 is available at
574 <https://www2.mmm.ucar.edu/wrf/src/WRFV3.7.1.TAR.gz>.

575 **Author contributions**

576 Zhongwei Luo: Data curation and collection, writing—original draft. Yan Han:
577 Modeling, writing—original draft. Kun Hua: Data collection. Yufen Zhang:
578 Supervision—Review & editing. Jianhui Wu: Supervision in source profile. Xiaohui Bi:
579 Supervision in source profile. Qili Dai: Resources. Baoshuang Liu: Resources. Yang
580 Chen: Modification and editing. Xin Long: Supervision in modeling. Yinchang Feng:
581 Supervision—Review & editing.

582 **Competing interests**

583 The authors declare that they have no known competing financial interests or
584 personal relationships that could have appeared to influence the work reported in this
585 paper.

586 **Disclaimer. Publisher's note**

587 Copernicus Publications remains neutral with regard to jurisdictional claims in
588 published maps and institutional affiliations.

589 **Acknowledgements**

590 We would like to thank the National Natural Science Foundation of China (grant
591 number 42177465) for providing funding for the project. We are grateful for the

592 Inventory Spatial Allocate Tool (ISAT) provided by Kun Wang from Department of Air
593 Pollution Control, Institute of Urban Safety and Environmental Science, Beijing
594 Academy of Science and Technology. We thank two anonymous referees, Astrid
595 Kerkweg (Executive Editor) and Klaus Klingmüller (Top Editor) for the time and effort
596 spent in reviewing the manuscript.

597 **Financial support**

598 This study was financially supported by the National Natural Science Foundation
599 of China (grant number 42177465).

600 **Reference**

- 601 Appel, K. W., Poullo, G. A., Simon, H., Sarwar, G., Pye, H. O. T., Napelenok, S. L., Akhtar, F., Roselle,
602 S. J.: Evaluation of dust and trace metal estimates from the Community Multiscale Air Quality
603 (CMAQ) model version 5.0, *Geosci. Model Dev.*, 6, 883-899, [https://doi.org/10.5194/gmd-6-883-](https://doi.org/10.5194/gmd-6-883-2013)
604 [2013](https://doi.org/10.5194/gmd-6-883-2013), 2013.
- 605 Bi, X., Dai, Q., Wu, J., Zhang, Q., Zhang, W., Luo, R., Cheng, Y., Zhang, J., Wang, L., Yu, Z., Zhang, Y.,
606 Tian, Y., Feng, Y.: Characteristics of the main primary source profiles of particulate matter across
607 China from 1987 to 2017, *Atmos. Chem. Phys.*, 19, 3223-3243, [https://doi.org/10.5194/acp-19-](https://doi.org/10.5194/acp-19-3223-2019)
608 [3223-2019](https://doi.org/10.5194/acp-19-3223-2019), 2019.
- 609 Cao, J., Qiu, X., Gao, J., Wang, F., Wang, J., Wu, J., Peng, L.: Significant decrease in SO₂ emission and
610 enhanced atmospheric oxidation trigger changes in sulfate formation pathways in China during
611 2008–2016, *J. Clean. Prod.*, 326, 129396, <https://doi.org/10.1016/j.jclepro.2021.129396>, 2021.
- 612 Chapel Hill, N.: Operational Guidance for the Community Multiscale Air Quality (CMAQ) Mo
613 deling System Version 5.0, https://www.airqualitymodeling.org/index.php/CMAQ_version_5.0
614 [February 2010 release](https://www.airqualitymodeling.org/index.php/CMAQ_version_5.0) OGD#Aerosol Module, last access: February 2012.
- 615 Chen, Z., Chen, D., Zhao, C., Kwan, M., Cai, J., Zhuang, Y., Zhao, B., Wang, X., Chen, B., Yang, J., Li,
616 R., He, B., Gao, B., Wang, K., Xu, B.: Influence of meteorological conditions on PM_{2.5}
617 concentrations across China: A review of methodology and mechanism, *Environ. Int.*, 139, 105558,
618 <https://doi.org/10.1016/j.envint.2020.105558>, 2020.
- 619 Cheng, N. L., Meng, F., Wang, J. K., Chen, Y. B., Wei, X., Han, H.: Numerical simulation of the spatial
620 distribution and deposition of PM_{2.5} in East China coastal area in 2010 (In Chinese), *Journ. Safety*
621 *Environ.*, 15, 305-310, <https://doi.org/10.13637/j.issn.1009-6094.2015.06.063>, 2015.
- 622 Foley, K. M., Roselle, S. J., Appel, K. W., Bhawe, P. V., Pleim, J., Otte, T., Mathur, R., Sarwar, G., Young,
623 J. O., Gilliam, R.: Incremental testing of the community multiscale air quality (CMAQ) modeling
624 system version 4.7, *Geosci. Model Dev.*, 3, 205-226, <https://doi.org/10.5194/gmd-3-205-2010>, 2010.
- 625 Fountoukis, C., Nenes, A.: ISORROPIA II: a computationally efficient thermodynamic equilibrium
626 model for K⁺-Ca²⁺-Mg²⁺-NH₄⁺-Na⁺-SO₄²⁻-NO₃⁻-Cl⁻-H₂O aerosols, *Atmos. Chem. Phys.*, 7,
627 4639-4659, <https://doi.org/10.5194/acp-7-4639-2007>, 2007.
- 628 Fu, X., Wang, S., Zhao, B., Xing, J., Cheng, Z., Liu, H., Hao, J.: Emission inventory of primary pollutants

629 and chemical speciation in 2010 for the Yangtze River Delta region, China, *Atmos. Environ.*, 70,
630 39-50, <https://doi.org/10.1016/j.atmosenv.2012.12.034>, 2013.

631 Fu, X., Wang, S. X., Chang, X., Cai, S., Xing, J., Hao, J. M.: Modeling analysis of secondary inorganic
632 aerosols over China: pollution characteristics, and meteorological and dust impacts, *Sci. Rep.*, 6,
633 35992, <https://doi.org/10.1038/srep35992>, 2016.

634 Gao, S., Zhang, S., Che, X., Ma, Y., Chen, X., Duan, Y., Fu, Q., Wang, S., Zhou, B., Wei, C., Jiao, Z.:
635 New understanding of source profiles: Example of the coating industry, *J. Clean. Prod.*, 357, 132025,
636 <https://doi.org/10.1016/j.jclepro.2022.132025>, 2022.

637 Guo, R., Yang, J., Liu, Z.: Influence of heat treatment conditions on release of chlorine from Datong coal,
638 *J. Anal. Appl. Pyrol.*, 71, 179-186, [https://doi.org/10.1016/S0165-2370\(03\)00086-X](https://doi.org/10.1016/S0165-2370(03)00086-X), 2004.

639 Guo, Y. Y., Gao, X., Zhu, T. Y., Luo, L., Zheng, Y.: Chemical profiles of PM emitted from the iron and
640 steel industry in northern China, *Atmos. Environ.*, 150, 187-197,
641 <https://doi.org/10.1016/j.atmosenv.2016.11.055>, 2017.

642 Guo, Z., Hao, Y., Tian, H., Bai, X., Wu, B., Liu, S., Luo, L., Liu, W., Zhao, S., Lin, S., Lv, Y., Yang, J.,
643 Xiao, Y.: Field measurements on emission characteristics, chemical profiles, and emission factors
644 of size-segregated PM from cement plants in China, *Sci. Total Environ.*, 151822,
645 <https://doi.org/10.1016/j.scitotenv.2021.151822>, 2021.

646 Han, Y., Xu, H., Bi, X. H., Lin, F. M., Li, J., Zhang, Y. F., Feng, Y. C.: The effect of atmospheric
647 particulates on the rainwater chemistry in the Yangtze River Delta, China, *J. Air Waste Manage.*, 69,
648 1452-1466, <https://doi.org/10.1080/10962247.2019.1674750>, 2019.

649 Hopke, P. K., Dai, Q., Li, L., Feng, Y.: Global review of recent source apportionments for airborne
650 particulate matter, *Sci. Total Environ.*, 740, 140091,
651 <https://doi.org/10.1016/j.scitotenv.2020.140091>, 2020.

652 Hopke, P. K., Feng, Y. C., Dai, Q.: Source apportionment of particle number concentrations: A global
653 review, *Sci. Total Environ.*, 819, 153104, <https://doi.org/10.1016/j.scitotenv.2022.153104>, 2022.

654 Hsu, Y., Divita, F., Dorn, J.: SPECIATE 5.0 - Speciation Database Development Documentation, Final
655 Report, M. MENETREZ, Abt Associates Inc./Office of Research and Development/U.S.
656 Environmental Protection Agency Research Triangle Park, NC27711,
657 https://www.epa.gov/sites/default/files/2019-07/documents/speciate_5.0.pdf, 2019.

658 Huang, C. H., Hu, J. L., Xue, T., Xu, H., Wang, M.: High-Resolution Spatiotemporal Modeling for
659 Ambient PM_{2.5} Exposure Assessment in China from 2013 to 2019, *Environ. Sci. Technol.*, 55, 2152-
660 2162, <https://doi.org/10.1021/acs.est.0c05815>, 2021.

661 Huang, Z. J., Zheng, J. Y., Qu, J. M., Zhong, Z. M., Wu, Y. Q., Shao, M.: A Feasible Methodological
662 Framework for Uncertainty Analysis and Diagnosis of Atmospheric Chemical Transport Models,
663 *Environ. Sci. Technol.*, 53, 3110-3118, <https://doi.org/10.1021/acs.est.8b06326>, 2019.

664 Ji, Z., Gan, M., Fan, X., Chen, X., Li, Q., Lv, W., Tian, Y., Zhou, Y., Jiang, T.: Characteristics of PM_{2.5}
665 from iron ore sintering process: Influences of raw materials and controlling methods, *J. Clean. Prod.*,
666 148, 12-22, <https://doi.org/10.1016/j.jclepro.2017.01.103>, 2017.

667 Li, J., Wu, Y., Ren, L., Wang, W., Tao, J., Gao, Y., Li, G., Yang, X., Han, Z., Zhang, R.: Variation in PM_{2.5}
668 sources in central North China Plain during 2017–2019: Response to mitigation strategies, *J.*
669 *Environ. Manage.*, 28, 112370, <https://doi.org/10.1016/j.jenvman.2021.112370>, 2021.

670 Li, M., Hu, M., Du, B., Guo, Q., Tan, T., Zheng, J., Huang, X., He, L., Wu, Z., Guo, S.: Temporal and
671 spatial distribution of PM_{2.5} chemical composition in a coastal city of Southeast China, *Sci. Total*
672 *Environ.*, 605-606, 337-346, <https://doi.org/10.1016/j.scitotenv.2017.03.260>, 2017a.

673 Li, M., Liu, H., Geng, G., Hong, C., Liu, F., Song, Y., Tong, D., Zheng, B., Cui, H., Man, H., Zhang, Q.,
674 He, K.: Anthropogenic emission inventories in China: a review, *Natl. Sci. Rev.*, 4, 834-866,
675 <https://doi.org/10.1093/nsr/nwy044>, 2017b.

676 Li, X., He, K., Li, C., Yang, F., Zhao, Q., Ma, Y., Chen, Y., Ouyang, W., Chen, G.: PM_{2.5} mass, chemical
677 composition, and light extinction before and during the 2008 Beijing Olympics, *J. Geophys. Res.*,
678 118, 12158-12167, <https://doi.org/10.1002/2013JD020106>, 2013.

679 Liang, F., Xiao, Q., Yang, X., Liu, F., Li, J., Lu, X., Liu, Y., Gu, D.: The 17-y spatiotemporal trend of
680 PM_{2.5} and its mortality burden in China, *Proc. Natl. Acad. Sci.*, 117, 25601-25608,
681 <https://doi.org/10.1073/pnas.1919641117>, 2020.

682 Lv, L., Wei, P., Li, J., Hu, J.: Application of machine learning algorithms to improve numerical simulation
683 prediction of PM_{2.5} and chemical components, *Atmos. Pollut. Res.*, 12, 101211,
684 10.1016/j.apr.2021.101211, 2021.

685 NBS (National Bureau of Statistics of China): China Statistical Yearbook 2021,
686 <http://www.stats.gov.cn/tjsj/ndsj/2021/indexch.htm>, last access: 2022.

687 Peterson, G., Hogrefe, C., Corrigan, A., Neas, L., Mathur, R., Rappold, A.: Impact of Reductions in
688 Emissions from Major Source Sectors on Fine Particulate Matter-Related Cardiovascular Mortality,
689 *Environ. Health Persp.*, 128, 017005, <https://doi.org/10.1289/EHP5692>, 2020.

690 Qi, H., Cui, C., Zhao, T., Bai, Y., Liu, L.: Numerical simulation on the characteristics of PM_{2.5} heavy
691 pollution and the influence of weather system in Hubei Province in winter 2015 (In Chinese),
692 *Meteorological monthly*, 45, 1113-1122, <https://doi.org/10.7519/j.issn.1000-0526.2019.08.008>,
693 2019.

694 Seinfeld, J. H., Pandis, S. N.: Atmospheric Chemistry and Physics, from air pollution to climate change.
695 John Wiley & Sons, Inc., Hoboken, New Jersey.47-61, ISBN9781119221166, 2006

696 Sha, T., Ma, X., Jia, H., Tian, R., Chang, Y., Cao, F., Zhang, Y.: Aerosol chemical component: Simulations
697 with WRF-Chem and comparison with observations in Nanjing, *Atmos. Environ.*, 218, 1-14,
698 <https://doi.org/10.1016/j.atmosenv.2019.116982>, 2019.

699 Shi, W., Liu, C., Norback, D., Deng, Q., Huang, C., Qian, H., Zhang, X., Sundell, J., Zhang, Y., Li, B.,
700 Kan, H., Zhao, Z.: Effects of fine particulate matter and its constituents on childhood pneumonia: a
701 cross-sectional study in six Chinese cities, *Lancet*, 392, S79, [https://doi.org/10.1016/S0140-](https://doi.org/10.1016/S0140-6736(18)32708-9)
702 [6736\(18\)32708-9](https://doi.org/10.1016/S0140-6736(18)32708-9), 2018.

703 Shi, Z., Li, J., Huang, L., Wang, P., Wu, L., Ying, Q., Zhang, H., Lu, L., Liu, X., Liao, H., Hu, J.: Source
704 apportionment of fine particulate matter in China in 2013 using a source-oriented chemical transport
705 model, *Sci. Total Environ.*, 601-602, 1476-1487, <https://doi.org/10.1016/j.scitotenv.2017.06.019>,
706 2017.

707 Song, S. Y., Wang, Y. S., Wang, Y. L., Wang, T., Tan, H. Z.: The characteristics of particulate matter and
708 optical properties of Brown carbon in air lean condition related to residential coal combustion,
709 *Powder Technol.*, 379, 505-514, <https://doi.org/10.1016/j.powtec.2020.10.082>, 2021.

710 Tang, X. Y., Zhang, Y. H., Shao, M.: Atmosphere Environment Chemistry, Second ed (In Chinese). .
711 Higher Education Press, Beijing, China.268-329, ISBN978-7-04-019361-9, 2006

712 Wang, C., Zheng, J., Du, J., Wang, G., Klemes, J., Wang, B., Liao, Q., Liang, Y.: Weather condition-
713 based hybrid models for multiple air pollutants forecasting and minimisation, *J. Clean. Prod.*, 352,
714 131610, <https://doi.org/10.1016/j.jclepro.2022.131610>, 2022.

715 Wang, D., Hu, J., Xu, Y., Lv, D., Xie, X., Kleeman, M., Xing, J., Zhang, H., Ying, Q.: Source
716 contributions to primary and secondary inorganic particulate matter during a severe wintertime

717 PM_{2.5} pollution episode in Xi'an, China, *Atmos. Environ.*, 97, 182-194,
718 <https://doi.org/10.1016/j.atmosenv.2014.08.020>, 2014.

719 Weagle, C., Sinder, G., Li, C. C., Donkelaar, A., S, P., Bissonnette, P., Burke, I., Jackson, J., Latimer, R.,
720 Stone, E., Abboud, I., Akoshile, C., Anh, N., Brook, J., Cohen, A., Dong, J., Gibson, M., Griffith,
721 D., He, K., Holben, B., Kahn, R., Keller, C., Kim, J., Lagrosas, N., Lestari, P., Khian, Y., Liu, Y.,
722 Marais, E., Martins, J., Misra, A., Muliane, U., Pratiwi, R., Quel, E., Salam, A., Segey, L., Tripathi,
723 S., Wang, C., Zhang, Q., Brauer, M., Rudich, Y., Martin, R.: Global Sources of Fine Particulate
724 Matter: Interpretation of PM_{2.5} Chemical Composition Observed by SPARTAN using a Global
725 Chemical Transport Model, *Environ. Sci. Technol.*, 52, 11670-11681,
726 <https://doi.org/10.1021/acs.est.8b01658>, 2018.

727 Wongphatarakul, V., Friedlander, S. K., Pinto, J. P.: A Comparative Study of PM_{2.5} Ambient Aerosol
728 Chemical Databases, *Environ. Sci. Technol.*, 32, 3926-3934, <https://doi.org/10.1021/es9800582>,
729 1998.

730 Wu, B., Bai, X., Liu, W., Zhu, C., Hao, Y., Lin, S., Liu, S., Luo, L., Liu, X., Zhao, S., Hao, J., Tian, H.:
731 Variation characteristics of final size-segregated PM emissions from ultralow emission coal-fired
732 power plants in China, *Environ. Pollut.*, 259, 113886, <https://doi.org/10.1016/j.envpol.2019.113886>,
733 2020.

734 Wu, D., Zheng, H., Li, Q., Jin, L., Lyu, R., Ding, X., Huo, Y., Zhao, B., Jiang, J., Chen, J., Li, X., Wang,
735 S.: Toxic potency-adjusted control of air pollution for solid fuel combustion, *Nat. Energy*, 7, 194-
736 202, <https://doi.org/10.1038/s41560-021-00951-1>, 2022.

737 Wu, Z. X., Hu, T. F., Hu, W., Shao, L. Y., Sun, Y. Z., Xue, F. L., Niu, H. Y.: Evolution in physicochemical
738 properties of fine particles emitted from residential coal combustion based on chamber experiment,
739 *Gondwana Res.*, <https://doi.org/10.1016/j.gr.2021.10.017>, 2021.

740 Xia, Z. Q., Fan, X. L., Huang, Z. J., Liu, Y. C., Yin, X. H., Ye, X., Zheng, J. Y.: Comparison of Domestic
741 and Foreign PM_{2.5} Source Profiles and Influence on Air Quality Simulation (In Chinese), *Res.*
742 *Environ. Sci.*, 30, 359-367, <https://doi.org/10.13198/j.issn.1001-6929.2017.01.55>, 2017.

743 Yang, F., Tan, J., Zhao, Q., Du, Z., He, K., Ma, Y., Duan, F., Chen, G., Zhao, Q.: Characteristics of PM_{2.5}
744 speciation in representative megacities and across China, *Atmos. Chem. Phys.*, 11, 1025-1051,
745 <https://doi.org/10.5194/acpd-11-1025-2011>, 2011.

746 Ying, Q., Feng, M., Song, D. L., Wu, L., Hu, J., Zhang, H., Kleeman, M., Li, X.: Improve regional
747 distribution and source apportionment of PM_{2.5} trace elements in China using inventory-observation
748 constrained emission factors, *Sci. Total Environ.*, 624, 355-365,
749 <https://doi.org/10.1016/j.scitotenv.2017.12.138>, 2018.

750 Yu, Z. C., Jang, M., Kim, S., Bae, C., Koo, B., Beardsley, R., Park, J., Chang, L., Lee, H., Lim, Y., Cho,
751 J.: Simulating the Impact of Long-Range-Transported Asian Mineral Dust on the Formation of
752 Sulfate and Nitrate during the KORUS-AQ Campaign, *Earth Space Chem.*, 4, 1039-1049,
753 <https://doi.org/10.1021/acsearthspacechem.0c00074>, 2020.

754 Zhang, J., Wu, J., Lv, R., Song, D., Huang, F., Zhang, Y., Feng, Y.: Influence of Typical Desulfurization
755 Process on Flue Gas Particulate Matter of Coal-fired Boilers (In Chinese), *Environ. Sci.*, 41, 4455-
756 4461, <https://doi.org/10.13227/j.hjxx.202003193>, 2020.

757 Zhang, Q., Xue, D., Wang, S., Wang, L., Wang, J., Ma, Y., Liu, X.: Analysis on the evolution of PM_{2.5}
758 heavy air pollution process in Qingdao (In Chinese), *China Environ. Sci.*, 37, 3623-3635,
759 <https://doi.org/10.3969/j.issn.1000-6923.2017.10.003>, 2017.

760 Zhang, S. P., Xing, J., Sarwar, G., Ge, Y. L., He, H., Duan, F., Zhao, Y., He, K., Zhu, L., Chu, B.:

761 Parameterization of heterogeneous reaction of SO₂ to sulfate on dust with coexistence of NH₃ and
762 NO₂ under different humidity conditions, *Atmos. Environ.*, 208, 133-140,
763 <https://doi.org/10.1016/j.atmosenv.2019.04.004>, 2019.

764 Zheng, B., Tong, D., Li, M., Liu, F., Hong, C., Geng, G., Li, H., Li, X., Peng, L., Qi, J., Yan, L., Zhang,
765 Y., Zhao, H., Zheng, Y., He, K., Zhang, Q.: Trends in China's anthropogenic emissions since 2010
766 as the consequence of clean air actions, *Atmos. Chem. Phys.*, 18, 14095-14111,
767 <https://doi.org/10.5194/acp-18-14095-2018>, 2018.

768 Zheng, B., Zhang, Q., Zhang, Y., He, K. B., Wang, K., Zheng, G. J., Duan, F. K., Ma, Y. L., Kimoto, T.:
769 Heterogeneous chemistry: a mechanism missing in current models to explain secondary inorganic
770 aerosol formation during the January 2013 haze episode in North China, *Atmos. Chem. Phys.*, 15,
771 2031–2049, 10.5194/acp-15-2031-2015, 2015.

772 Zheng, H., Song, S., Sarwar, G., Gen, M., Wang, S., Ding, D., Chang, X., Zhang, S., Xing, J., Sun, Y. L.,
773 Ji, D., Chan, C. K., Gao, J., McElroy, M.: Contribution of Particulate Nitrate Photolysis to
774 Heterogeneous Sulfate Formation for Winter Haze in China, *Environ. Sci. Technol. Lett.*, 7, 632-
775 638, <https://doi.org/10.1021/acs.estlett.0c00368>, 2020.

776 Zhou, L., Chen, X., Tian, X.: The impact of fine particulate matter (PM_{2.5}) on China's agricultural
777 production from 2001 to 2010, *J. Clean. Prod.*, 178, 133-141,
778 <https://doi.org/10.1016/j.jclepro.2017.12.204>, 2018.

779